

Phenomenology of Absolute Neutrino Masses

Carlo Giunti^a

^aINFN, Sezione di Torino, and Dipartimento di Fisica Teorica, Università di Torino, Via P. Giuria 1, I-10125 Torino, Italy

The phenomenology of absolute neutrino masses is reviewed, focusing on tritium β decay, cosmological measurements and neutrinoless double- β decay. Talk presented at NOW-2004, Neutrino Oscillation Workshop, 11–17 September 2004, Conca Specchiulla, Otranto, Italy.

1. Introduction

Solar, atmospheric and long-baseline neutrino oscillation experiments obtained convincing evidence that neutrinos are massive and mixed particles. Since on one hand solar and KamLAND experiments and on the other hand atmospheric and K2K experiments are sensitive to oscillations generated by different orders of magnitude of differences of squared neutrino masses, at least two independent $\Delta m_{\text{SUN}}^2 \ll \Delta m_{\text{ATM}}^2$ are needed in order to explain the data. This requirement is satisfied by the simplest three-neutrino mixing scheme in which the left-handed components $\nu_{\alpha L}$ of flavor neutrinos ($\alpha = e, \mu, \tau$) are linear combinations of the left-handed components ν_{kL} of massive neutrinos ($k = 1, 2, 3$): $\nu_{\alpha L} = \sum_k U_{\alpha k} \nu_{kL}$, where U is the unitary mixing matrix (see, for example, Ref. [1, 2, 3]). In such framework neutrino oscillations depend on two independent squared-mass differences Δm_{21}^2 and Δm_{31}^2 , that we associate by convention to the squared-mass differences that are effective in solar and atmospheric neutrino oscillations, respectively: $\Delta m_{21}^2 = \Delta m_{\text{SUN}}^2$ and $|\Delta m_{31}^2| = \Delta m_{\text{ATM}}^2$. The absolute value of Δm_{31}^2 is needed because two type of schemes, shown in Fig.1, are allowed by the observed hierarchy $\Delta m_{\text{SUN}}^2 \ll \Delta m_{\text{ATM}}^2$. In the normal scheme, which is so-called because it allows a mass hierarchy $m_1 \ll m_2 \ll m_3$, Δm_{31}^2 is positive, whereas in the inverted scheme Δm_{31}^2 is negative.

A global fit of the data [4] gives the best-fits and 3σ ranges for the three-neutrino oscillation parameters listed in Tab.1. The mixing angles ϑ_{12} , ϑ_{13} , ϑ_{23} belong to the standard parameterization of the mixing matrix [5], in which with

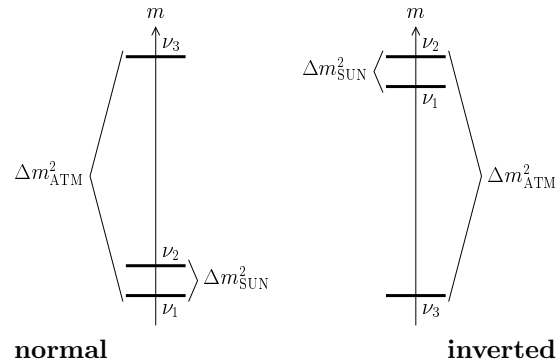


Figure 1. The two three-neutrino schemes allowed by the hierarchy $\Delta m_{\text{SUN}}^2 \ll \Delta m_{\text{ATM}}^2$.

good approximation ϑ_{12} is the solar mixing angle, ϑ_{23} is the atmospheric mixing angle, and ϑ_{13} is the CHOOZ mixing angle [6, 7]. In Tab.1 we give only the measured values of ϑ_{12} and ϑ_{13} obtained in the global fit of Ref. [4], which are sufficient for the following discussion on the phenomenology of absolute neutrino masses.

Neutrino oscillations depend on the difference of neutrino masses, not on their absolute value. As we will see in the following, other experiments are able to give information on the absolute value of neutrino masses. Figure 2 shows the values of the neutrino masses obtained from Δm_{21}^2 and $|\Delta m_{31}^2|$ in Tab.1 as functions of the unknown lightest mass, which is m_1 in the normal scheme and m_3 in the inverted scheme. As shown in the figure, the case $m_3 \ll m_1 \lesssim m_2$ is conventionally called “inverted hierarchy”, whereas in both normal and inverted schemes we have quasi-

Table 1

Best-fit and 3σ range for the three-neutrino oscillation parameters obtained in the global fit of Ref. [4].

| Parameter | Best-Fit 3σ Range |
|-------------------------|---|
| Δm_{21}^2 | $8.3 \times 10^{-5} \text{ eV}^2$ $7.4 \times 10^{-5} - 9.3 \times 10^{-5} \text{ eV}^2$ |
| $\sin^2 \vartheta_{12}$ | 0.28 0.22 - 0.37 |
| $ \Delta m_{31}^2 $ | $2.4 \times 10^{-3} \text{ eV}^2$ $1.8 \times 10^{-3} - 3.2 \times 10^{-3} \text{ eV}^2$ |
| $\sin^2 \vartheta_{13}$ | 0.01 0 - 0.05 |

degeneracy of neutrino masses for $m_1 \simeq m_2 \simeq m_3 \gg \sqrt{\Delta m_{\text{ATM}}^2} \simeq 5 \times 10^{-2} \text{ eV}$.

In the following we review the phenomenology of absolute neutrino masses in tritium β decay (Section 2), cosmological measurements (Section 3) and neutrinoless double- β decay (Section 4).

2. Tritium β Decay

The measurement of the electron spectrum in β decays provides a robust direct determination of the values of neutrino masses. In practice the most sensitive experiments use tritium β decay, because it is a super-allowed transition with a low Q -value. Information on neutrino masses is obtained by measuring the Kurie function $K(T)$ given by [8, 9, 10]

$$K^2(T) = (Q - T) \sum_k |U_{ek}|^2 \sqrt{(Q - T)^2 - m_k^2},$$

where T is the electron kinetic energy. The effect of neutrino masses can be observed near the end point of the electron spectrum where $Q - T \sim m_k$. A low Q -value is important because the relative number of events occurring in an interval of energy ΔT below the end-point is $\propto (T/Q)^3$.

Since the present experiments do not see any effect due to neutrino masses, it is possible to

approximate $m_k \ll Q - T$ and obtain

$$K^2(T) \simeq (Q - T) \sqrt{(Q - T)^2 - m_\beta^2}, \quad (1)$$

which is a function of only one parameter, the effective neutrino mass [8, 9, 10, 11, 12, 13, 14]

$$m_\beta^2 = \sum_k |U_{ek}|^2 m_k^2. \quad (2)$$

The current best upper bounds on m_β are given by the Mainz and Troitsk experiments (see Ref. [15]), which obtained the same value

$$m_\beta < 2.2 \text{ eV} \quad (95\% \text{ CL}). \quad (3)$$

In the future the KATRIN experiment [16] will reach a sensitivity of about 0.2 eV.

In the standard parameterization of the mixing matrix we have ($c_{ij} \equiv \cos \vartheta_{ij}$ and $s_{ij} \equiv \sin \vartheta_{ij}$)

$$m_\beta^2 = c_{12}^2 c_{13}^2 m_1^2 + s_{12}^2 c_{13}^2 m_2^2 + s_{13}^2 m_3^2. \quad (4)$$

Since the values of Δm_{21}^2 , $|\Delta m_{31}^2|$, ϑ_{12} and ϑ_{13} are determined by neutrino oscillation experiments, there is only one unknown quantity in Eq.(4), which corresponds to the absolute scale of neutrino masses. Figure 3 shows the value of m_β as a function of the unknown lightest mass, which is m_1 in the normal scheme and m_3 in the inverted scheme, using the values of the oscillation parameters in Tab.1. The middle solid lines correspond to the best fit and the extreme solid lines delimit the 3σ allowed range. We have also shown with dashed lines the 3σ ranges of the neutrino masses (same as in Fig.2), which help to understand their contribution to m_β . One can see that in the case of a normal mass hierarchy (normal scheme with $m_1 \ll m_2 \ll m_3$) the main contribution to m_β can be due to m_2 or m_3 or both, because the upper limit for m_β is larger than the upper limit for m_2 . In the case of an inverted mass hierarchy (inverted scheme with $m_3 \ll m_1 \lesssim m_2$) m_β has practically the same value as m_1 and m_2 .

Figure 3 shows that the Mainz and Troitsk experiments and the future KATRIN experiment give information on the absolute values of neutrino masses in the quasi-degenerate region in both normal and inverted schemes. In the far future the inverted scheme could be excluded if experiments with a sensitivity of about $4 \times 10^{-2} \text{ eV}$ will not find any effect of neutrino masses.

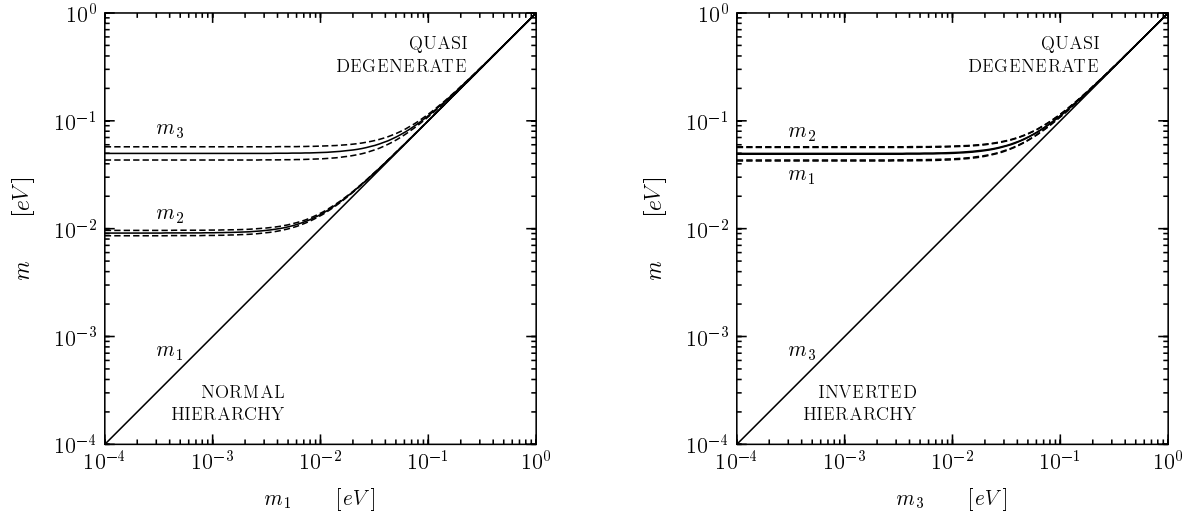


Figure 2. Values of neutrino masses as functions of the lightest mass m_1 in the normal scheme and m_3 in the inverted scheme. Solid lines correspond to the best-fit in Tab. 1. Dashed lines enclose 3σ ranges.

3. Cosmological Measurements

If neutrinos have a mass of the order of 1 eV they constitute a so-called “hot dark matter”, which suppresses the power spectrum of density fluctuations in the early universe at “small” scales of the order of 1–10 Mpc (see Ref. [17]). The suppression depends on the sum of neutrino masses $\sum_k m_k$.

Recent high precision measurements of density fluctuations in the Cosmic Microwave Background (WMAP) and in the Large Scale Structure of galaxies (2dFGRS, SDSS), combined with other cosmological data have allowed to put stringent upper limits on $\sum_k m_k$ [18,19,20,21,22,23,4]. However, different authors have obtained significantly different upper bounds mainly because of the different sets of data considered. The most crucial data are the so-called Lyman- α forests which are constituted by absorption lines in the spectra of high-redshift quasars due to intergalactic hydrogen clouds. Since these clouds have dimensions of the order of 1–10 Mpc, the Lyman- α data are crucial in order to push the upper bound on $\sum_k m_k$ below 1 eV. Unfortunately the interpretation of Lyman- α data may suffer from large systematic uncertainties. Summarizing the different limits obtained in Refs. [18,19,20,21,22,23,4],

we estimate the approximate 2σ upper bounds

$$\sum_k m_k \lesssim 0.5 \text{ eV}, \quad \sum_k m_k \lesssim 1 \text{ eV}, \quad (5)$$

with and without Lyman- α data, respectively. From Fig 4 one can see that both these limits constrain the neutrino masses in the quasi-degenerate region, where the upper bound on each individual mass is one third of the bound on the sum. In the future the inverted scheme can be excluded by an upper bound of about 8×10^{-2} eV on the sum of neutrino masses.

4. Neutrinoless Double- β Decay

Neutrinoless double- β decay is a very important process because it is not only sensitive to the absolute value of neutrino masses, but mainly because it is allowed only if neutrinos are Majorana particles [24,25]. A positive result in neutrinoless double- β decay would represent a discovery of a new type of particles, Majorana particles, a fundamental improvement in our understanding of nature.

Neutrinoless double- β decays are processes of type $\mathcal{N}(A, Z) \rightarrow \mathcal{N}(A, Z+2) + e^- + e^-$, in which no neutrino is emitted, with a change of two units of the total lepton number. These processes, for-

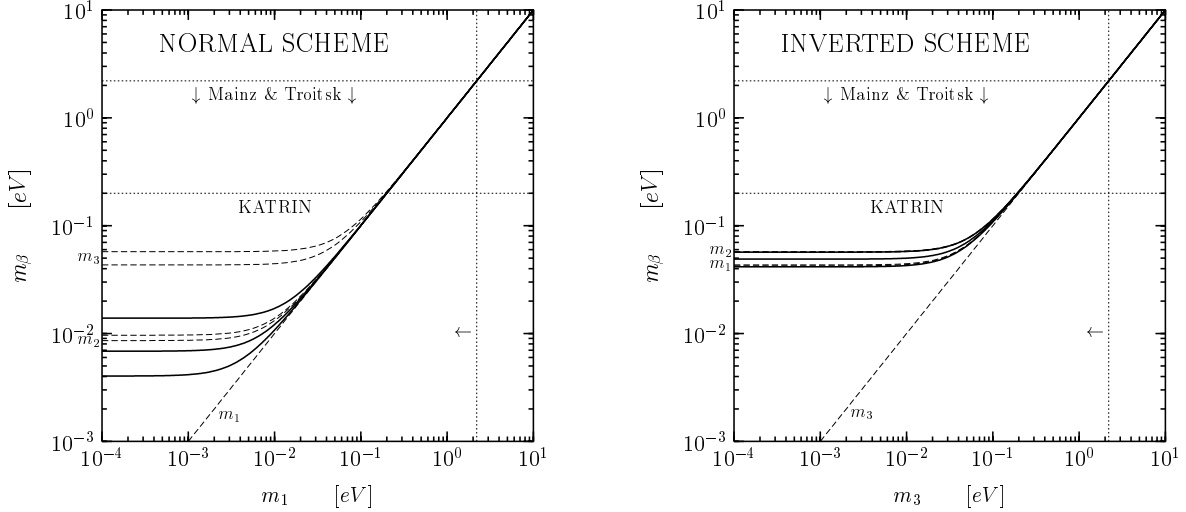


Figure 3. Effective neutrino mass m_β in tritium β -decay experiments as a function of the lightest mass m_1 in the normal scheme and m_3 in the inverted scheme. Middle solid lines correspond to the best-fit in Tab. 1. Extreme solid lines enclose 3σ ranges. Dashed lines delimit 3σ ranges of individual masses.

bidden in the Standard Model, have half-lives

$$T_{1/2}^{0\nu} = (G_{0\nu} |\mathcal{M}_{0\nu}|^2 |m_{\beta\beta}|^2)^{-1}, \quad (6)$$

where $G_{0\nu}$ is the phase-space factor, $\mathcal{M}_{0\nu}$ is the nuclear matrix element and

$$m_{\beta\beta} = \sum_k U_{ek}^2 m_k \quad (7)$$

is the effective Majorana mass.

A possible indication of neutrinoless double- β decay of ^{76}Ge with half-life

$$T_{1/2}^{0\nu}(^{76}\text{Ge}) = (0.69 - 4.18) \times 10^{25} \text{ y} \quad (3\sigma) \quad (8)$$

has been found by the authors of Ref. [26], whereas other experiments found only lower bounds. The most stringent lower bound on $T_{1/2}^{0\nu}(^{76}\text{Ge})$ has been obtained in the Heidelberg-Moscow experiment [27]:

$$T_{1/2}^{0\nu}(^{76}\text{Ge}) > 1.9 \times 10^{25} \text{ y} \quad (90\% \text{ CL}). \quad (9)$$

The IGEX experiment [28] obtained the comparable limit $T_{1/2}^{0\nu}(^{76}\text{Ge}) > 1.57 \times 10^{25} \text{ y}$ (90% CL). Hence, the status of the experimental search for neutrinoless double- β decays is presently uncertain and new experiments which can check the indication (8) are needed (see Ref. [29]).

The extraction of the value of $|m_{\beta\beta}|$ from the data has unfortunately a serious problem due to the large theoretical uncertainty in the evaluation of the nuclear matrix element $\mathcal{M}_{0\nu}$ (see Refs. [30, 29]). In the following we will use as “ 3σ ” range for the nuclear matrix element $|\mathcal{M}_{0\nu}|$ the interval which covers the results of reliable calculations listed in Tab.2 of Ref. [29] (other approaches are discussed in Refs. [31, 32, 33, 4]):

$$0.41 \lesssim |\mathcal{M}_{0\nu}| \lesssim 1.24, \quad (10)$$

which corresponds to a “ 3σ ” uncertainty of a factor of 3 for the determination of $|m_{\beta\beta}|$ from $T_{1/2}^{0\nu}(^{76}\text{Ge})$. Using the range (10), the indication (8) implies

$$0.22 \text{ eV} \lesssim |m_{\beta\beta}| \lesssim 1.6 \text{ eV}, \quad (11)$$

and the most stringent upper bound (9) implies

$$|m_{\beta\beta}| \lesssim 0.32 - 1.0 \text{ eV}. \quad (12)$$

In the standard parameterization of the mixing matrix the effective Majorana mass is given by

$$m_{\beta\beta} = c_{12}^2 c_{13}^2 m_1 + s_{12}^2 c_{13}^2 e^{i\alpha_{21}} m_2 + s_{13}^2 e^{i\alpha_{31}} m_3,$$

where α_{21} and α_{31} are unknown Majorana phases (see, for example, Ref. [1, 2, 3]).

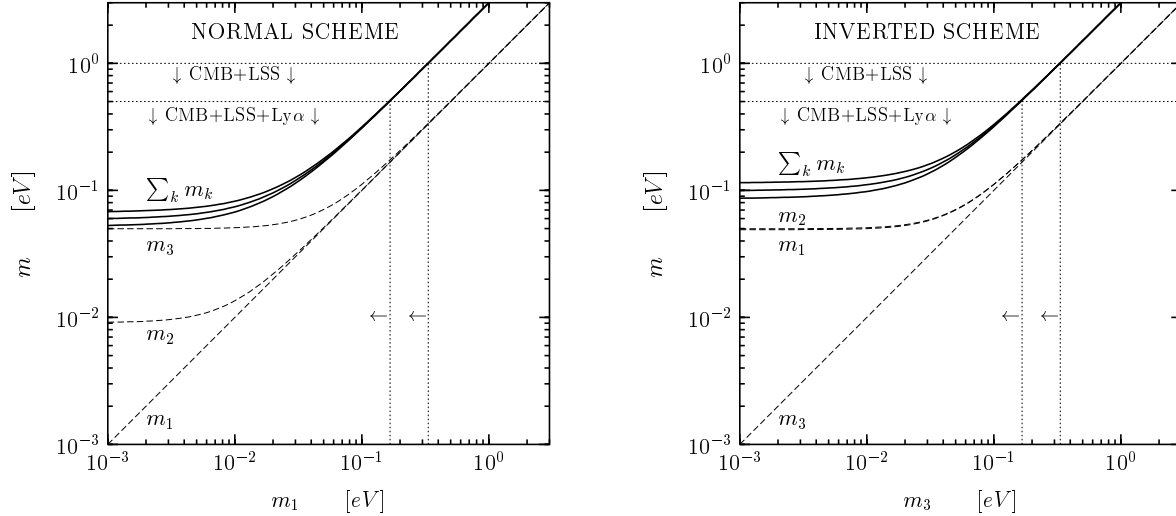


Figure 4. Sum of neutrino masses as a function of the lightest mass m_1 in the normal scheme and m_3 in the inverted scheme. Middle solid lines correspond to the best-fit in Tab. 1. Extreme solid lines enclose 3σ ranges. Dashed lines show the best-fit values of individual masses.

Figure 5 shows the allowed range for $|m_{\beta\beta}|$ obtained with the mixing parameters in Tab.1 (see also Refs. [34, 35, 36, 3, 32, 37, 38]). One can see that in the region where the lightest mass is very small the allowed ranges for $|m_{\beta\beta}|$ in the normal and inverted schemes are dramatically different. This is due to the fact that in the normal scheme strong cancellations between the contributions of m_2 and m_3 are possible, whereas in the inverted scheme the contributions of m_1 and m_2 cannot cancel because maximal mixing in the 1–2 sector is excluded by solar data ($\vartheta_{12} < \pi/4$ at 5.8σ [39]). On the other hand, there is no difference between the normal and inverted schemes in the quasi-degenerate region, which is probed by the present data. From Fig.5 one can see that there is a tension between the indication (11) and the cosmological upper bound on individual neutrino masses, especially the one with Lyman- α data. In the future, the normal and inverted schemes may be distinguished by reaching a sensitivity of about 10^{-2} eV.

5. Conclusions

In conclusion we would only like to emphasize the fundamental importance of the determination

of the Dirac or Majorana nature of neutrinos and their absolute mass scale. Improvements on these topics should be strongly pursued in future experimental and theoretical research.

REFERENCES

1. S.M. Bilenky, C. Giunti and W. Grimus, Prog. Part. Nucl. Phys. 43 (1999) 1.
2. S.M. Bilenky et al., Phys. Rep. 379 (2003) 69.
3. C. Giunti and M. Laveder, hep-ph/0310238.
4. G.L. Fogli et al., hep-ph/0408045.
5. Particle Data Group, S. Eidelman et al., Phys. Lett. B592 (2004) 1.
6. S.M. Bilenky and C. Giunti, Phys. Lett. B444 (1998) 379, hep-ph/9802201.
7. W.L. Guo and Z.Z. Xing, Phys. Rev. D67 (2003) 053002, hep-ph/0212142.
8. R.E. Shrock, Phys. Lett. B96 (1980) 159.
9. B.H.J. McKellar, Phys. Lett. B97 (1980) 93.
10. I.Y. Kobzarev et al., Sov. J. Nucl. Phys. 32 (1980) 823.
11. E. Holzschuh, Rep.Prog.Phys. 55 (1992) 1035.
12. Mainz, C. Weinheimer et al., Phys. Lett. B460 (1999) 219.
13. F. Vissani, Nucl. Phys. Proc. Suppl. 100 (2001) 273, hep-ph/0012018.

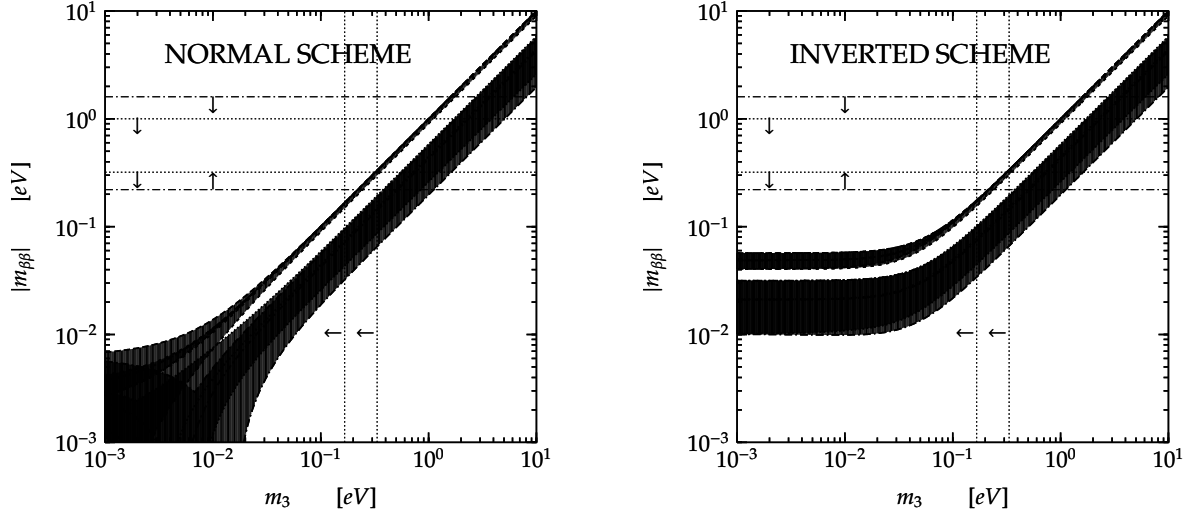


Figure 5. Effective Majorana mass $|m_{\beta\beta}|$ in neutrinoless double- β decay experiments as a function of the lightest mass m_1 in the normal scheme and m_3 in the inverted scheme. The white areas in the strips need CP violation. The horizontal dotted lines show the interval (12) of uncertainty of the current experimental upper bound due to the estimated uncertainty (10) of the value of the nuclear matrix element. The horizontal dash-dotted lines delimit the range (11) obtained from the indication (8). The vertical dotted lines correspond to the cosmological upper bounds on individual neutrino masses in Fig.4.

14. Y. Farzan and A.Y. Smirnov, Phys. Lett. B557 (2003) 224, [hep-ph/0211341](#).
15. C. Weinheimer, [hep-ex/0210050](#).
16. KATRIN, L. Bornschein et al., eConf C030626 (2003) FRAP14.
17. W. Hu et al., Phys. Rev. Lett. 80 (1998) 5255, [astro-ph/9712057](#).
18. D.N. Spergel et al., Ast. J. Supp. Ser. 148 (2003) 175, [astro-ph/0302209](#).
19. S. Hannestad, JCAP 0305 (2003) 004, [astro-ph/0303076](#).
20. O. Elgaroy and O. Lahav, JCAP 04 (2003) 004, [astro-ph/0303089](#).
21. SDSS, M. Tegmark et al., Phys. Rev. D69 (2004) 103501, [astro-ph/0310723](#).
22. U. Seljak et al., [astro-ph/0406594](#).
23. U. Seljak et al., [astro-ph/0407372](#).
24. J. Schechter and J.W.F. Valle, Phys. Rev. D25 (1982) 2951.
25. E. Takasugi, Phys. Lett. B149 (1984) 372.
26. H. Klapdor-Kleingrothaus et al., Phys. Lett. B586 (2004) 198, [hep-ph/0404088](#).
27. H.V. Klapdor-Kleingrothaus et al., Eur. Phys. J. A12 (2001) 147.
28. IGEX, C.E. Aalseth et al., Phys. Rev. D65 (2002) 092007, [hep-ex/0202026](#).
29. S.R. Elliott and J. Engel, J. Phys. G30 (2004) R183, [hep-ph/0405078](#).
30. O. Civitarese and J. Suhonen, Nucl. Phys. A729 (2003) 867, [nucl-th/0208005](#).
31. V.A. Rodin et al., Phys. Rev. C68 (2003) 044302, [nucl-th/0305005](#).
32. S. Bilenky, A. Faessler and F. Simkovic, Phys. Rev. D70 (2004) 033003, [hep-ph/0402250](#).
33. J.N. Bahcall, H. Murayama and C. Pena-Garay, Phys. Rev. D70 (2004) 033012, [hep-ph/0403167](#).
34. F. Feruglio, A. Strumia and F. Vissani, Nucl. Phys. B659 (2003) 359, [hep-ph/0201291](#).
35. F.R. Joaquim, Phys. Rev. D68 (2003) 033019.
36. S. Pascoli and S.T. Petcov, Phys. Lett. B580 (2004) 280, [hep-ph/0310003](#).
37. J.N. Bahcall et al., Phys. Rev. D70 (2004) 033012, [hep-ph/0403167](#).
38. S.T. Petcov, New J. Phys. 6 (2004) 109.
39. J.N. Bahcall et al., JHEP 08 (2004) 016, [hep-ph/0406294](#).